Performance of Water-based Liquid Scintillator

D. Beznosko[c,], M.V. Diwan[a], S.Hans[b], D. Jaffe[a], S.H. Kettell[a], R.Rosero[b],
H. Themann[a], B. Viren[a], E. Worcester[a], M. Yeh[b], C. Zhang[a]

[a]*Physics Department, Brookhaven National Laboratory, Upton, NY 11973, USA*
[b]*Chemistry Department, Brookhaven National Laboratory, Upton, NY 11973, USA*
[c]*Department of Physics, Nazarbayev University, Astana, 010000, KZ*

Abstract

The Water-based Liquid Scintillator (WbLS) is a new material currently under development. It is based on the idea of dissolving the organic scintillator in water using special surfactants. This material strives to achieve the novel detection techniques by combining the Cerenkov rings and scintillation light, as well as the total cost reduction compared to pure liquid scintillator (LS).

Presented are the light yield measurements for the three different proton beam energies (210MeV, 475MeV and 2000MeV) for water, two different WbLS formulations (0.4% and 0.99%) and pure LS. The results show that a goal of 100 optical photons/MeV, indicated by the simulation to be an optimal light yield for observing both the Cerenkov ring and scintillation light from the proton decay in a large water detector, has been achieved.

Keywords: Water based, liquid scintillator, beam test

1. Motivation

In large water detectors, the Cerenkov radiation produced by a charged particle above the threshold can be used for particle identification, and the reconstruction of its direction and energy [1]. However, all charged particles below the Cerenkov threshold are missed. Detecting these below-threshold particles is important for various applications. For example, in the search of the proton decay, in the $p^+ \rightarrow K^+\overline{\nu}$ channel, where K$^+$ is mostly below Cerenkov threshold and is invisible is a water detector. The use of the WbLS

---

makes the kaon visible and allows for the separation of K^+, μ^+ and e^+ signals using timing and reduce background for this decay channel.

In either LS or WbLS, the isotropic scintillation light is produced by the charged particle energy deposition via ionization, but the scintillator components may interfere with the Cerenkov ring detection. To detect K^+ and preserve the Cerenkov ring, MC studies indicate that the light yield (LY) from the scintillator component int he WbLS should be 100 optical photons/MeV.

Thus, WbLS potentially combines both the Cerenkov ring and scintillation light capabilities. It can preserve the particle identification for the particles above the Cerenkov threshold, and detect the charged particles below the threshold via the scintillation light. In addition, WbLS features the lower cost than pure LS and it is safer to handle[ask Minfang for reference].

The ability to reach the desired LY can be checked using the mono-energetic proton beam with different WbLS concentrations. For the test, the two different WbLS formulations (0.4% and 0.99%), pure water and pure LS samples were chosen. Three different proton beam energies were used with each sample. The choice of the energies comes from the following considerations:

- 2000MeV protons behave as minimum ionizing particle (MIP)

- 475MeV protons are just below the Cerenkov limit in water

- 210MeV protons have ~same energy deposition as K^+ from the proton decay channel mentioned above.

2. Experimental Setup

The experimental setup used for the proton beam test is shown in Figure 1. Two tubs with the samples were used (T1 and T2). Three 2cm x 2cm 5mm thick plastic scintillator hodoscopes were used (H1 to H3) with the beam trigger being formed by the coincidence of the H1&H2 only. H3 was intended to verify whether particles exit T2. .

2.1. Tub and Signal Readout Description

Two tubs were used in the experiment:

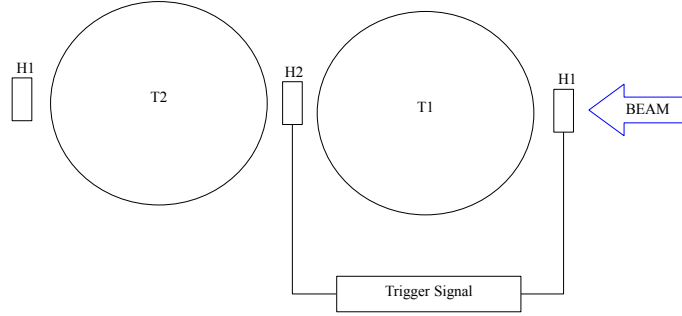- T1 from Polytetrafluoroethylene (PTFE) (white, highly reflective),

Figure 1: Proton beam test experimental setup.

- T2 from Aluminum, coated with black PTFE (very low reflectivity).

The T1 allows the capture of most of the light produced in the tub, whereas T2 allows for the observation of the light coming directly from the scintillation without the multiple wall reflections. An image of a tub is in Figure 3. Both T1 and T2 have the same dimensions:

- the lid is 19.05mm thick,

- the walls and bottom are 6.35mm thick,

- inner height and diameter are 150mm.

.

A detailed setup readout scheme is shown in Figure 2. Both tubs were read out by Hamamatsu [2] R7723 2" Photo-multiplier tubes (PMT). An acrylic window transparent for the ultraviolet light (UVT) was used as a partition between the PMT and the liquid in the tub. The window was protruding through the lid and into the liquid by several millimeters to ensure that there are no air bubbles on its surface.

A readout was by the 4-channel 14bit CAEN [3] V1729A Flash Analog-to-Digital Converter (FADC). All tubs signals were connected to the FADC via a
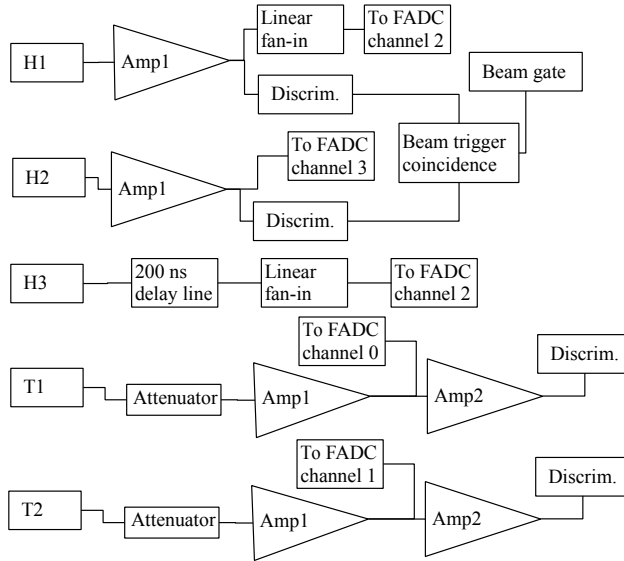
Figure 2: Proton beam test experimental setup.

⁵⁸ variable attenuation unit (Phillips Scientific [4] 804) and a variable amplifier
⁵⁹ unit (Phillips Scientific 778). For the T1 and the T2 readouts, the gain was
⁶⁰ set to the values of ∼2x. The first output from the amplifier goes to the
⁶¹ FADC, with a dedicated channel for each tub. The second output from each
⁶² amplifier channel was used for the single photo-electron (PE) calibration.
⁶³ The gain for the second amplification stage was set at ∼10x.

⁶⁴ All hodoscopes also were connected via ∼2x gain amplifier channels that
⁶⁵ allows signal splitting. H1 and H3 shares the same FADC channel with
⁶⁶ latter signal being delayed by 200ns. H2 was connected to the last remaining
⁶⁷ channel of the FADC.

⁶⁸ *2.2. Triggering Scheme*

⁶⁹ Triggering schema was realized using three 2cm x 2cm, 5mm thick plastic
⁷⁰ scintillator counters that were readout by 2" PMTs via an air waveguide
⁷¹ in order to remove the PMTs from direct beam exposure. The signal from
⁷² the front-most and a middle counters were used to form a bean trigger, as
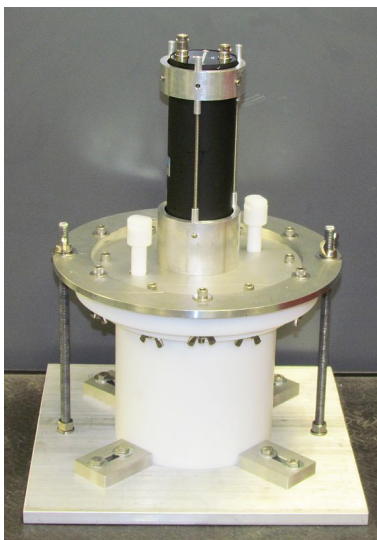⁷³ indicated in the Figure 2.

4

Figure 3: PTFE tub detector with a PMT.

2.3. Proton Beamline Description

A proton test beam was conducted at NASA Space Radiation Laboratory (NSRL) facility at BNL. As described above, the three proton beam energies were used: 210MeV, 475MeV and 2GeV. The beam had the following main characteristics:

- intensity of $\sim$1p$^+$/bunch,

- beam size was 1cm x1cm at 2GeV and 5.4cm x 5.4cm at 210MeV,

- 0.4s long spills every $\sim$4 sec.

3. Data Analysis

3.1. Liquids Measured

???? how much details? this is a question to chemists. 4 samples tested:

- Water (purified)

- WbLS-1: 0.4%LS

- WbLS-2: 0.99%LS

5

- LS: 100% LS

- OR

- Water (purified)

- WbLS-1: 0.4%PC +0.4g/L PPO+3mg/L MSB+surfactant in water

- WbLS-2: 0.99%PC +1.36g/L PPO+7.48mg/L MSB+surfactant in water

- LS: LAB + 2g/L PPO + 15mg/L MSB.

3.2. Waveform Analysis

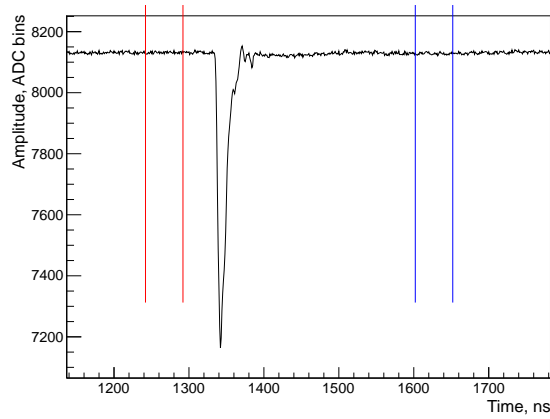Figure 4: Typical PMT waveform with baseline check windows.

The PMT signal is acquired as a waveform shown in Figure 4. Total acquisition window is 2560 bins per event with each bin being 1ns wide; the signal is approximately centered and the approximate position is known beforehand. A 300ns window (central one in the figure, between the red and blue lines) is used to obtain the integrated signal area by summation. Each point is subtracted from the average baseline to achieve a positive sum. A typical signal is smaller then the chosen window width, however, there is a small spread in timing of the signals and we want' to be sure that all of the signal has been integrated. The size of the chosen window is the same for all samples and measurements.
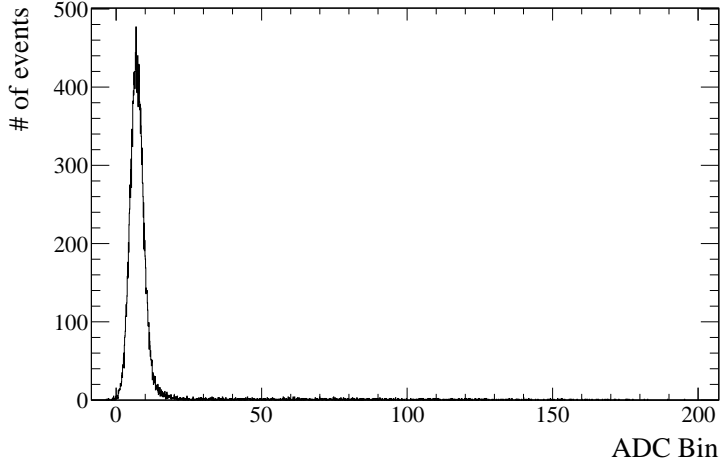
6

Figure 5: Typical baseline value for a single channel.

A baseline is defined as the average value of all the points in the first integration window (between the two red lines) that is 50ns wide. A typical baseline is shown in Figure 5 To check the baseline quality, its averaged value is compared against the average of the post-signal window (between two blue lines). This difference is illustrated in Figure 6. Events with this difference larger then $\sim$20 ADC bins are flagged as bad. This allows for the removal of the noise events or events with the bad baseline. Additionally, a comparison of the baseline with an average of a window at the very beginning of the waveform (between 10ns and 40ns, not shown because the figure is zoomed around the signal area) is used for general baseline quality check using the above criterion.

The integrated area is a measure of total charge that can be converted to the PE yield using the single PE calibration of the PMTs. This allows to describe the measured signals independent of the hardware differences between the channels.

The trigger information that is saved in the two additional FADC channels allows for the offline trigger requirements be used.

3.3. Single Photo Electron Calibration

A single PE calibration was conducted for both signal channels at the end of the test beam run. For it, the trigger is produced from the discriminator that follows the second amplifier for the T1 and T2 signals (separately for
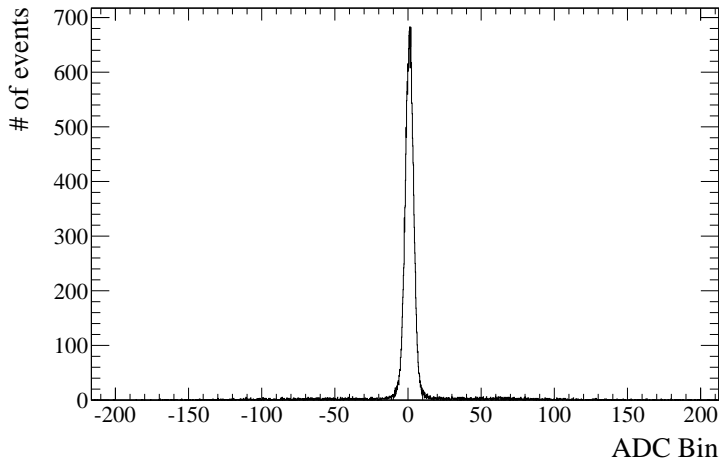
7

Figure 6: Difference between the baseline and the average of the post-signal window.

each, see Figure 2). The discriminator is set to $\sim 1/10^{\text{th}}$ of the single PE amplitude as to allows for better PE signal detection efficiency than using random trigger. Additionally, this forces the PE signal to the signal window region of the FADC output for the simplified analysis and elimination of the partially captured signals. Note that a PE signal is much narrower and lower in amplitude/area then the beam signals that are typically many PEs that arrive with time distribution, thus a smaller integration window is used to reduce noise for cleaner calibration (50ns instead of 300ns).

The signal area calibration is 168.0±1.2 ADC bins and 132.9±1.6 ADC bins for T1 and T2 respectively (the PE signal is summed within the window, so the unit of ADC bin is still used). A special care was taken to separately verify that this method yields the same calibration values as using the light-emitting diode (LED) scheme. For that, calibration runs using the described above scheme and using the dim LED pulses were compared to each other. The LED light level is chosen such that only $\sim 1/10^{\text{th}}$ of the events has the single PE signal to insure that these are the single photon detection responses.

3.4. Data quality selection

The data quality selection is done as a single step before the data is analyzed. The care was taken to choose the criteria that do not introduce a bias into the selection. These are:

8

₁₄₇ • offline double trigger requirement for H1 and H2 to be above ∼50mV
₁₄₈ and within the expected time window,

₁₄₉ • baseline quality check as outlines in chapter 3.2,

₁₅₀ • ADC saturation check for H1 and H2.

₁₅₁ Each check is intended to remove potential noise or multiple particles
₁₅₂ in an event. The saturation check indicates if several particles have passed
₁₅₃ thought the hodoscopes in a same beam spill that happens rarely at the
₁₅₄ intensity used.

₁₅₅ *3.5. Light Yield Results*
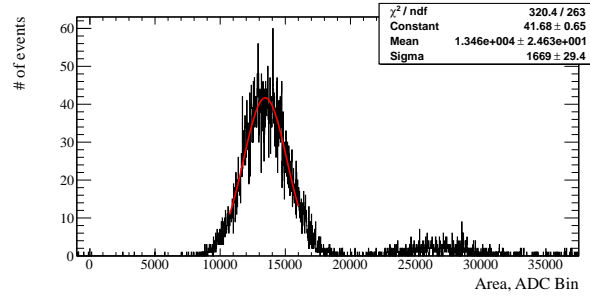

Figure 7: A sample fit of a tub signal.

₁₅₆ For each sample and energy, a histogram of the signal areas is computed.
₁₅₇ A fit using a Gaussian and a bin likelihood method is then performed. The
₁₅₈ fitting is done in two steps - first, a Gaussian is fitted in the range between the
₁₅₉ half of the maximum peak values to obtain the first approximation. Then,
₁₆₀ the fits around the found mean with 1, 1.5 and 2σ are carried. This is
₁₆₁ done to estimate the uncertainty that the fit width is adding because of the
₁₆₂ second peak due to the two particles passing through the tub during the
₁₆₃ same trigger time. Figure 7 shows the 1.5σ fit of the single particle fit, and
₁₆₄ the two-particle peak is visible on it as well. This plot is in the ADC bins
₁₆₅ for clarity; single-PE calibration will be applied to all further plots.
₁₆₆ The data for all the samples at all energies is then processed in the same
₁₆₇ way. Plots in Figure 8 and in Figure 9 show the light yield results in PE
₁₆₈ for the different samples and beam energies for Tub1 and tub2 respectively.
₁₆₉ Note that the LS light yield values plotted are reduced by a factor of 30.

9

In addition, the data point for the LS at 210MeV for T1 is not going to be shown on firther plots because of the readout saturation due to large light amount.

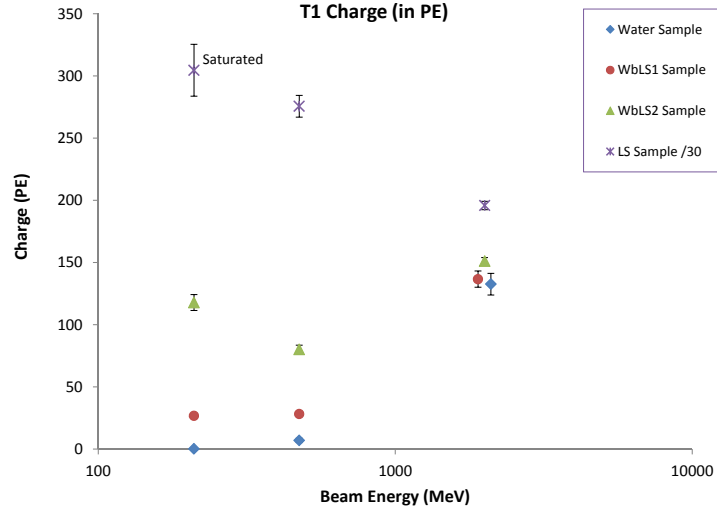Figure 8: The light yield in PE for T1. At 2GeV beam energy, some points are offset for clarity.

3.6. Energy deposition

In order to estimate the PE/MeV light yield of each sample, the energy deposition in each sample is needed. Two methods were used for this purpose: a GEANT4 simulation of the beamline setup with the deposition being the mean of the 1000 runs at each energy, and a simplified code that would calculate the proton energy loss along a straight line path through the tubs and hodoscopes with small steps, using the proton stopping power and range tables (PSTAR) from the National Institute of Standards and Technology (NIST). The WbLS was modeled as water, and the LS as toluene.

The resulting energy depositions are listed in Table 1. The difference between the two methods is taken as the uncertainty for the values obtained (summed as square root of the sum of the squares with the RMS of the mean). The converted into the PE/MeV light yield is shown in Figure 10 for the T1 and in Figure 11 for the T2.
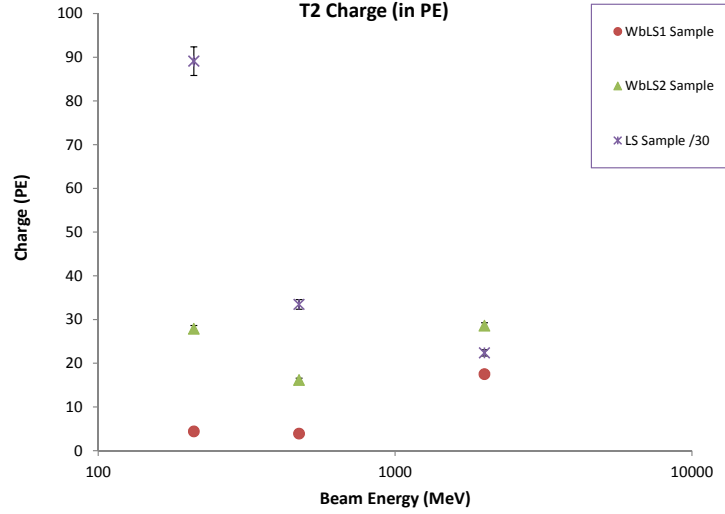
Figure 9: The light yield in PE for T2.

3.7. Systematics

asdf

3.7.1. Calibration Stability

4. Conclusion

References

[1] M. Fechner et.al. (The Super-Kamiokande Collaboration),'Kinematic reconstruction of atmospheric neutrino events in a large water Cherenkov detector with proton identification', Phys. Rev. D 79 (2009) 112010, arXiv:0901.1645

[2] Hamamatsu Photonics, 314-5 Shimokanzo, Toyooka-village, Iwatagun, Shizuoka-ken, 438-0193 Japan; http://www.hamamatsu.com

[3] CAEN (Costruzioni Apparecchiature Elettroniche Nucleari S.p.A.), Via della Vetraia 11, 55049 Viareggio, Province of Lucca, Italy, 0584 388398.

[4] Phillips Scientific, 31 Industrial Ave. Suite 1, Mahwah, N.J. 07430

11

Table 1: Energy Deposition in Samples

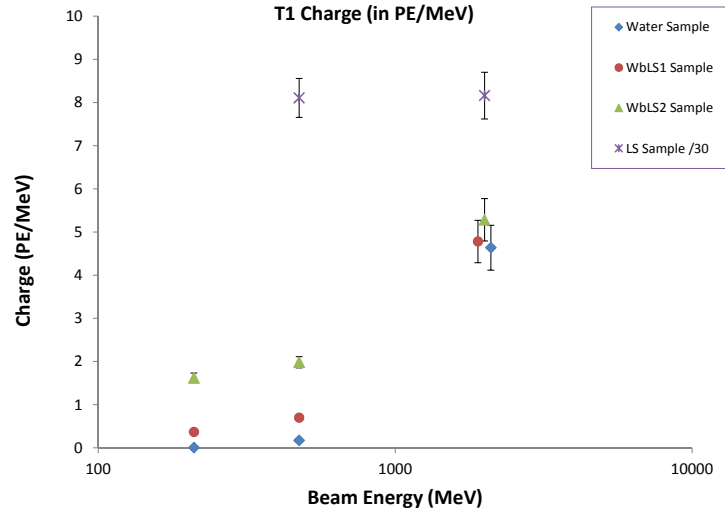| Beam Energy (MeV)	Sample	T1 Energy Deposit (MeV)	T2 Energy Deposit (MeV)
210	Water, WbLS	72.7±3.1	107.5±6.1
	LS	59±	124±
475	Water, WbLS	40.4±2.0	43.7±2.2
	LS	34±	36±
2000	Water, WbLS	28.6±2.6	28.7±3.1
	LS	24±	24±

Figure 10: The light yield in PE/MeV for T1. At 2GeV beam energy, some points are offset for clarity.
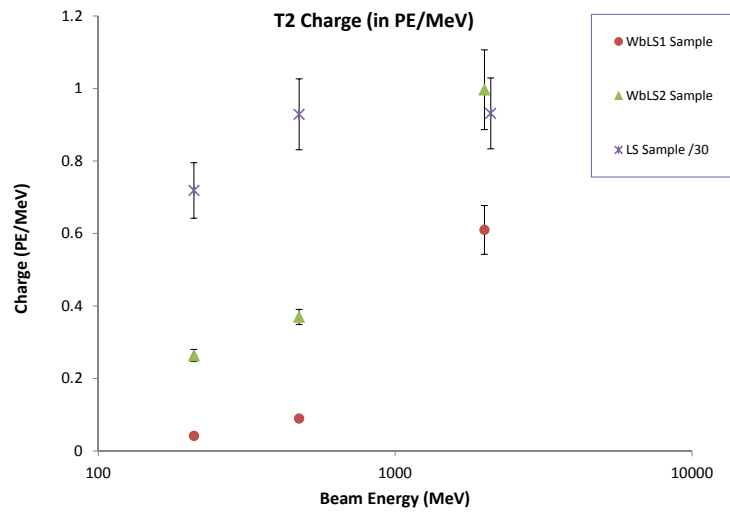
Figure 11: The light yield in PE/MeV for T2. At 2GeV beam energy, some points are offset for clarity.